Electrically Conductive Polyaniline–Poly(vinyl alcohol) Composite Films: Physical Properties and Morphological Structures

Show-An Chen* and Woei-Guwn Fang

Chemical Engineering Department, National Tsing-Hua University, Hsinchu, Taiwan 30043, China

Received June 12, 1990; Revised Manuscript Received August 7, 1990

ABSTRACT: Polyaniline (PAn)–poly(vinyl alcohol) (PVA) composite film prepared electrochemically has a gradient of PAn content along the thickness direction with some PVA chains grafted by PAn chains to various extents along the thickness direction. This composite film can be considered to be composed of four regions: a PAn layer, a PAn-rich region, a PAn gradient region, and a PAn-poor region. The composite film has conductivities on the film surface of the electrode side about equal to the conductivity of PAn at the same doping level and on the solution side lower than the conductivity of PAn by a factor of 10^4. As a result of the PAn content gradient and the presence of moisture, the bulk conductivity of the composite film drops significantly in the glass transition range of PVA. The chemically prepared composite film has a bulk conductivity lower than that of PAn by a factor of 10 with no significant variation in conductivity in the glass transition region of PVA and is featureless in morphology.

Introduction

Polyaniline (PAn) is an important conducting polymer because of its good environmental stability. It can be synthesized by polymerizing aniline in protonic acid aqueous solution in the presence of an oxidant such as ammonium peroxydisulfate or potassium dichromate[1,2] or in a protonic acid aqueous or organic solvent solution under a constant voltage[3] or potential cycling.[4,5] PAn synthesized by the former method is a black-green precipitate, but PAN synthesized by the latter method (using H_2SO_4 as the protonic acid) forms a dense smooth thin film (strongly adhered to the electrode surface) covered with a loosely packed layer.[6,7] This electrochemically produced film is brittle and cannot be peeled off to form a free-standing film. It was found by one of us[8] that this loosely packed layer has a fibrilar network morphology if tetrafluoroboric acid (HBF_4) is used and has a granular (or short pillar) morphology if HCl or H_2SO_4 is used.

Incorporating plastic or rubber with a conducting polymer is a promising method to introduce flexibility and toughness into conducting polymers, especially for PAn for which preparation of a free-standing film requires much effort.[9] For polypyrrole (PPy), composite films have been prepared by electrochemical polymerization on an electrode coated with a solvent-swellable insulating plastic film such as poly(vinyl chloride) (PVC)[10,11] or vinylidene fluoride–trifluoroethylene copolymer (PVDF–TrFE).[11,12] Another method[13,14] to produce PPy composite film is to expose an oxidizing-agent-impregnated plastic film to pyrrole vapor, allowing a polymerization of diffusing pyrrole molecules in the plastic substrate to form a composite film. Among these reports, only PPy/PVDF–TrFE[11,12] and PPy/PVC[11] composite films prepared by the electrochemical method were subjected to studies on morphological structure/property relationships. It was proposed that the composite films are of a layered structure and composed of three parts: (a) a PPy single layer, (b) a finely mixed layer, and (c) a coarsely mixed layer. For PAn, a composite film with polyester-based polyurethane (PU) has been prepared by electrochemical polymerization.[15] Morphological studies indicated that PAn particulates were dispersed in the PU substrate, and no chemical bonding between the two components was observed.

In this work, we report the morphological structure and physical properties of PAn/PVA composite films prepared electrochemically and chemically.

Experimental Section

1. **Chemicals.** Aniline and tetrafluoroboric acid were synthetic grade (Merck). PVA was BF-17 (Chung Chun Chemical Co., Taiwan) with hydrolysis 98.98% and $\bar{M}_w$ = 75 000.

2. **Electrochemical Polymerization.** An 8% by weight PVA aqueous solution was coated on one side of a 1 cm × 4 cm platinum (Pt) sheet, and the coated sheet was dried in an air stream for ~2 days to give a deposited film ~0.2 mm thick. Prior to the coating, the Pt sheet was cleaned by immersing in a mixture of concentric sulfuric acid and potassium dichromate aqueous solution to wash off residues on the surface, washing with distilled water, and finally oven-drying. Before synthesis, the PAn-coated side of the Pt sheet was treated with a thin layer of silicone grease to prevent electrochemical polymerization on its surface. The sheet was then immersed in deionized water for 10 min to allow swelling. With this PVA-coated Pt electrode as anode and another uncoated Pt sheet as cathode, a cell containing 1 M aniline and 1.2 M protonic acid (HBF_4) in deionized water was constructed. Electrochemical polymerization of aniline in the PVA coating on the anode was then carried out by applying an electrical potential of 1.1 V across the two electrodes for 1 h. A free-standing composite film was obtained by peeling it off from the electrode. Electrochemical polymerization of aniline on a PVA-free Pt sheet was also carried out under the same conditions.

3. **Chemical Polymerization.** An 8% by weight PVA aqueous solution was mixed with potassium dichromate aqueous solution. This mixed solution was then cast in a polyethylene trough and allowed to dry in an air stream for 3–5 days. The resulting orange-yellow cast film was ca. 0.1–0.25 mm thick and contained 20% potassium dichromate as oxidant. It was then dipped in an aqueous solution containing 1 M aniline and 1.2 M HBF_4. The aniline that diffused into the film was oxidized to form PAn. After 1 min, the film turned deep green and then darkened as the reaction proceeded further.

4. **Characterization.** For all physical measurements except the dynamic mechanical and conductivity measurements, the so-obtained PAn, PVA, and PAn/PVA composite from both methods were subjected to dynamic vacuum pumping for more than 48 h to remove residual moisture. For the dynamic mechanical and conductivity measurements, samples were only stored in a desiccator after their preparation in order to maintain flexibility of the film. Dried composite films are brittle and might break during the dynamic mechanical measurement.

* Author to whom correspondence should be addressed.

0024-9297/91/2224-1242$02.50/0 © 1991 American Chemical Society

Table I
Compositions of the PAn and PAn/PVA Composite Films

	chem method	electrochem method	
	PAn/PVA	PAn	PAn/PVA
PAn/PVA wt ratio[a]	1/4		1/1.2
X^b		0.54	0.42

[a] The weight of PAn does not include the weight of the dopant, HBF_4. [b] Mole fractions of HBF_4 per aniline unit.

(a)

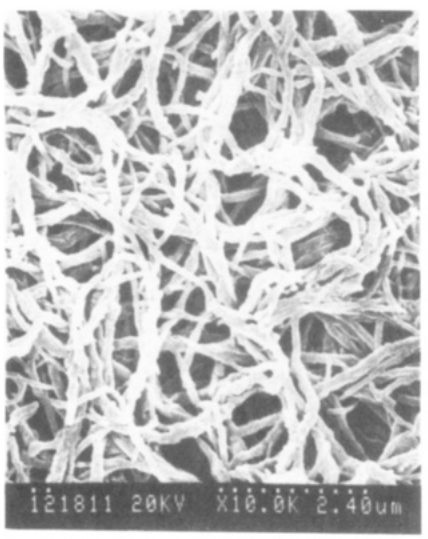

(b)

Figure 1. SEM micrographs of the PAn prepared by (a) the chemical method and (b) the electrochemical method.

An elemental analyzer (Perkin-Elmer Model 240C) was used to measure the amount of N and C, from which the weight ratio of PAn to PVA in the composite film was determined. Since the chemical formula of the PAn produced can be represented approximately by $[(C_6H_4NH)(HA)_y]_m$ and that of PVA by $(CH_2\text{-}CHOH)_m$, the weight fraction of PAn (X) excluding the incorporated protonic acid can be calculated from the following equation using the N/C weight ratio:

$$\frac{N}{C} = \frac{X(28/180)}{X(144/180) + (1 - X)28/44}$$

An inductively coupled plasma–atomic emission spectrometer (ICP–AES, Plasmakon Model S-35) was used to measure the amount of boron in the composite films and PAn. A 50-mg sample was digested in 3 mL of nitric acid in a pressure bomb at 150 °C for 4 h to give a clear solution and, after dilution, was fed into the cell of this instrument.

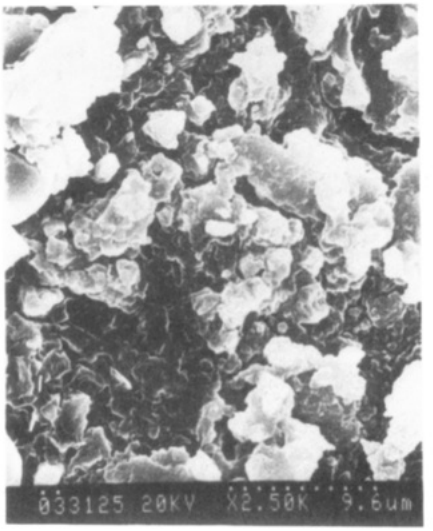

(a)

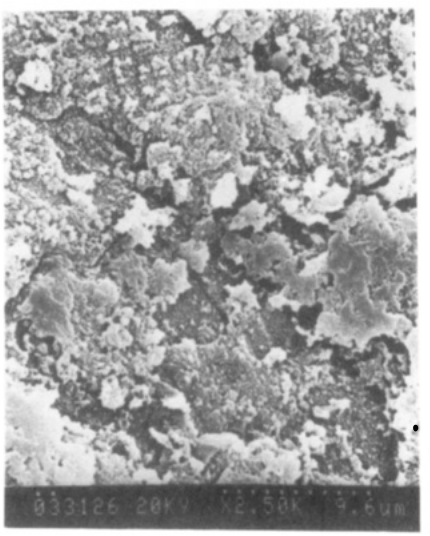

(b)

Figure 2. SEM micrographs of the surfaces of PAn/PVA films prepared by the chemical method: (a) unwashed; (b) washed with boiling water.

An infrared spectrophotometer (IR, Perkin-Elmer Model 983) was used to examine the interaction between PAn and PVA in the composite film. Specimens for PAn were prepared by grinding powdered PAn with KBr powder and then pressing the mixture into a tablet, while specimens for the electrochemically prepared composite films were obtained by allowing aniline to be polymerized for 3 min on the Pt anode coated with a thin film of PVA (10^{-3}-mm thickness) and then peeling the film off the electrode to give a transparent free-standing film having a green color.

A scanning electron microscope (SEM, Hitachi Model S-570) was used to examine the morphology of the composite films. A film of ca. 2 mm × 2 mm was fixed on the sample holder using an electroconductive adhesive and coated with a thin layer of gold about 400 Å in thickness to improve the SEM image resolution. To view the details of the dispersion of PAn in the composites, some of the composite films obtained from the chemical method were boiled in water for 2 h to remove the soluble parts of the PVA.

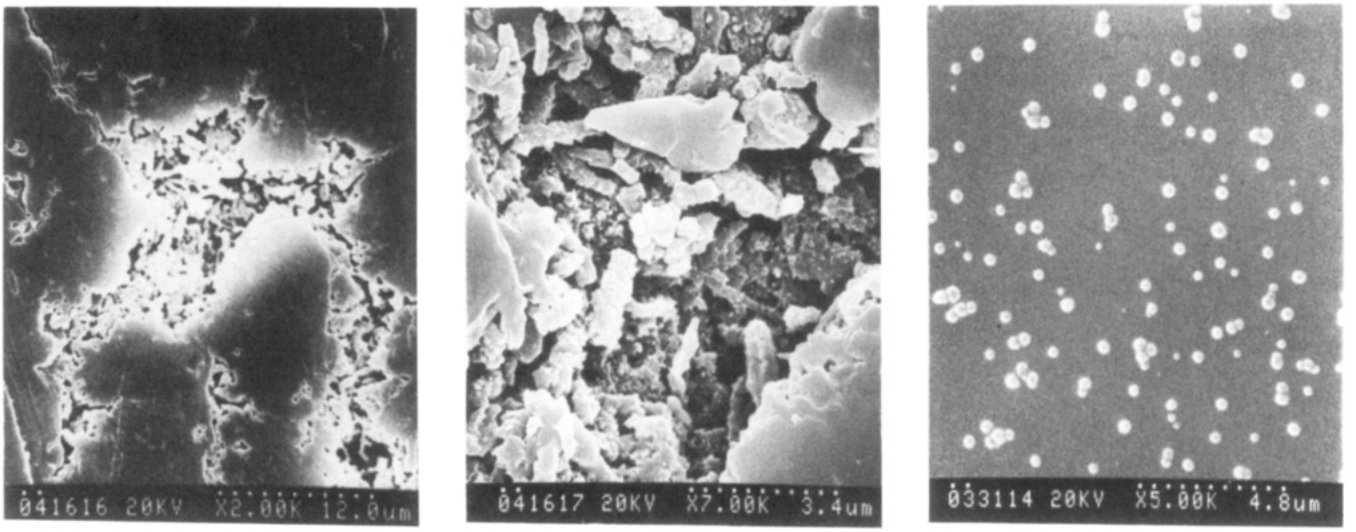

Figure 3. SEM micrographs of the surfaces of PAn/PVA films prepared by the electrochemical method: (a) the electrode side; (b) magnification of the broken area of (a); (c) the solution side.

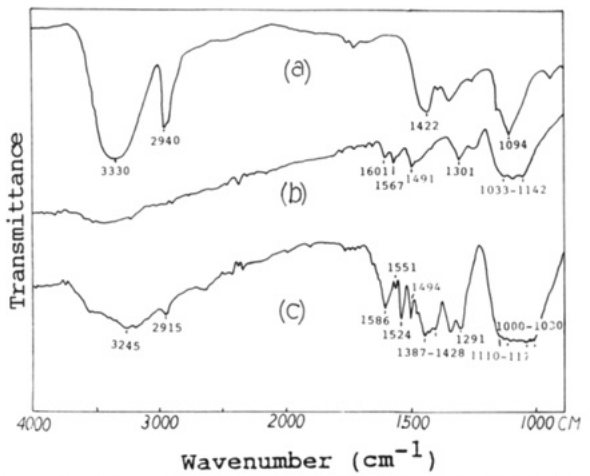

Figure 4. IR spectra of e-PAn, PVA, and e-PAn/PVA films: (a) PVA; (b) e-PAn; (c) e-PAn/PVA.

Table II
Characteristic Peaks (cm^{-1}) of the IR Spectra in Figure 4[a]

function group	PVA	e-PAn	e-PAn/PVA
O–H	3330		3245
C–H	2940		2915
C–O	1094		covered
CH_2	1422		1387–1428
C=C ring		1601, 1491	1586, 1494
C–N[b]		1301	1291
C=C ring of $IP^{\bullet+}$ [c]		1567	1551
			1524
BF_4^-		1033–1142	1033–1142
Ph–O of Ph–O–C			1110–1175
C–O of Ph–O–C			1000–1030

[a] All the frequencies are due to stretching vibration. [b] With aromatic conjugation of C. [c] $IP^{\bullet+}$ is radical cation of imino-1,4-phenylene.

A differential scanning calorimeter (DSC, Perkin-Elmer Model DSC-2C) was used to examine thermograms in the temperature range 50–400 °C with a heating rate of 20 °C/min.

A thermogravimetric analyzer (TGA, Perkin-Elmer Model TGS-2) was used to measure weight loss during the temperature scan from 50 to 450 °C with a heating rate of 20 °C/min.

A dynamic viscoelastometer (Toyo Baldwin Rheovibron DDV-II-EA) was used to measure the tensile and loss moduli ($|E^*|$ and E'') and loss tangent (tan δ) of the composite films in the temperature range −50 to +200 °C with a heating rate of 2 °C/min and a frequency of 110 Hz. The sample was ca. 20 mm long, 2 mm wide, and 0.25 mm thick.

A sandwich type four-probe method was used to measure the bulk conductivity of the composite films, a four-point apparatus (Alessi Industries) was used to measure the surface conductivities of both surfaces, and a two-disk method[16] was used to measure the conductivity along the film thickness direction. For measuring the bulk conductivity variation with temperature, the four-probe cell was inserted in a glass tube purged with nitrogen. The whole assembly was then immersed in liquid nitrogen cooling/oil bath heating surroundings having a temperature variation of ±0.5 °C to adjust the temperature. The temperature rise rate was kept about 3 °C/min.

Results and Discussion

1. Composition. Table I shows that, under the same concentrations of aniline and HBF_4 in the aqueous solution, the electrochemical method gives a much higher content of PAn in the composite film than the chemical method, even though the oxidant content in the PVA film was as high as 20 wt % in the chemical method. However, in the electrochemically prepared composite film, the PAn had a slightly lower doping level than that in the PAn prepared under the same conditions.

2. SEM Micrography. The PAn produced from the chemical method (c-PAn, where "c" refers to chemical) had a granular morphology (Figure 1a), while that produced from the electrochemical method had a fibrilar network morphology (diameter of the fibrils is about 0.24 μm, Figure 1b).

The PAn/PVA composite film produced from the chemical method (c-PAn/PVA) had a flakelike morphology (Figure 2a). After extraction with boiling water, the soluble portion of the PVA in the composite was dissolved in water, and the surface of the extracted composite shows a fine and loose granular morphology (Figure 2b).

The PAn/PVA composite film produced from the electrochemical method (e-PAn/PVA, where "e" refers to electrochemical) had a smooth surface on the electrode side (Figure 3a), under which the PAn is likely to be a fibrilar network dispersed in the PVA matrix as can be seen clearly from the broken parts of the surface (Figure 3a,b). The fibrils of the network were broken into short pillars, which could have been caused during the peeling off of the composite film from the electrode. On the

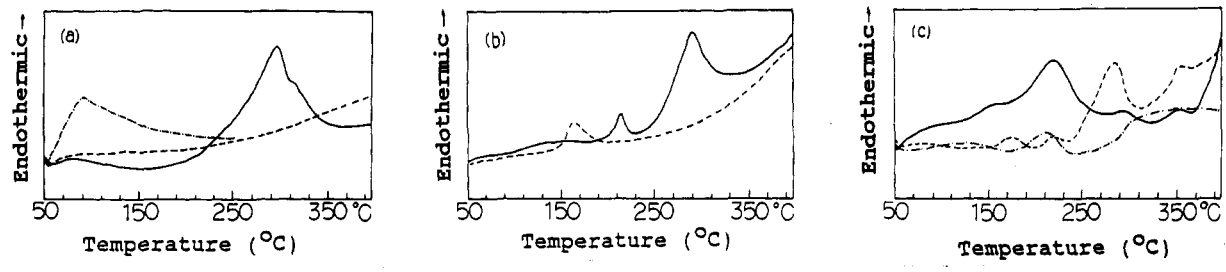

Figure 5. DSC curves of PAn, PVA, and PAn/PVA: (a) e-PAn (—), e-PAn without drying under vacuum (- · -), undoped e-PAn (- - -); (b) PVA (—), PVA treated with HBF_4 (- - -); (c) e-PAn/PVA (—), c-PAn/PVA (- - -), b-PAn/PVA (- · -).

solution side of the film, beads of PAn appear on the surface (Figure 3c), which were grown from the PAn fibrils dispersed in the interior of the PVA matrix.

3. Infrared Spectroscopy. IR spectra of PVA, e-PAn, and e-PAn/PVA composite film are shown in curves a, b, and c in Figure 4. The peak locations related to the corresponding chemical bonds are listed in Table II. For PVA, the characteristic absorption peaks are 3330 (O–H stretching), 2940 (C–H stretching), 1094 (C–O stretching), and 1422 cm^{-1} (CH_2 stretching). For PAn, the characteristic absorption peaks are[17-19] 1601 and 1491 C=C ring stretching), 1301 (C–N stretching), 1567 (C=C ring stretching of $IP^{\bullet+}$, where $IP^{\bullet+}$ is the radical cation of imino-1,4-phenylene), and 1033–1142 cm^{-1} (BF_4^-). A comparison of the spectrum for the composite film (Table II and Figure 4) with the spectra of the pure components PVA and e-PAn shows that the peak positions of all the above characteristic peaks except that of BF_4^- were shifted to lower wavenumbers. This indicates that hydrogen bonding between PVA and e-PAn occurs, which could result in a weakening in bond strength in PVA and e-PAn due to electron withdrawing.

In addition, new absorption peaks were observed in the ranges 1000–1030 and 1110–1175 cm^{-1} in the composite film. The absorption peaks in these ranges can be attributed to absorptions of C–O and Ph–O stretching vibrations in alkyl C–O–Ph.[20] Thus the new peaks would indicate a formation of the new linkage C–O–Ph, resulting from a grafting of PAn chain onto PVA chain. Furthermore, the absorption peak at 1567 cm^{-1} of $IP^{\bullet+}$ in PAn was split into two peaks, 1551 and 1524 cm^{-1}, in the composite films, which are attributed to the C=C ring stretching with and without the ether linkage, respectively, and provide additional evidence to support the existence of the newly generated ether linkage. In the absence of PVA, the former peak would be at higher wavenumber than 1567 cm^{-1} and the latter should remain unchanged (at 1567 cm^{-1}). The shifts to lower wavenumber of these two peaks are due to hydrogen bonding between the PAn and PVA.

4. Thermal Analysis. DSC and TGA measurements of PVA, e-PAn, and e- and c-PAn/PVA composite films prepared from the chemical and electrochemical methods are shown in Figures 5 and 6, respectively. The characteristic values of the DSC curves are listed in Table III. For e-PAn, a broad endothermic peak at 300 °C in the range 170–350 °C was observed in DSC (Figure 5a); after undoping by immersing the e-PAn in NH_4OH aqueous solution for 12 h to remove the acid, this peak was absent (Figure 5a). The TGA results (Figure 6a) show a continuous weight loss and a total weight loss of 15% at 350 °C, quite close to the weight percent of acid in the e-PAn, 14%. Thus this endothermic peak can be attributed to evaporation of the acid. For e-PAn without further drying under dynamic vacuum pumping, an additional endothermic peak at 96 °C appeared (Figure 5a); the TGA result

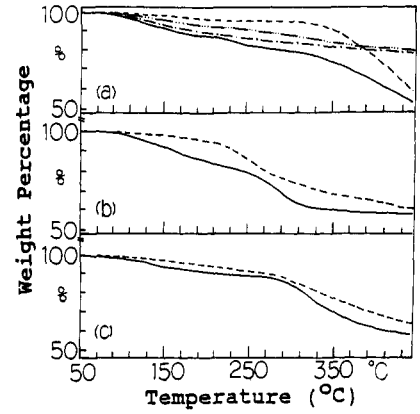

Figure 6. TGA curves of PVA, PAn, and PAn/PVA: (a) PAn without drying under vacuum (- · -), PAn after removal of water (- · ·), PVA without drying under vacuum (—), PVA after removal of water (- - -); (b) c-PAn/PVA without drying under vacuum (—), c-PAn/PVA after removal of water (- - -); (c) e-PAn/PVA without drying under vacuum (—), e-PAn/PVA after removal of water (- - -).

shows a steeper and higher percent weight loss before 150 °C (Figure 6a) than that of the vacuum-dried e-PAn. Thus the peak at 96 °C can be attributed to evaporation of water.

For PVA, two endothermic peaks were observed in DSC (Figure 5b), one at 220 °C in the range 200–230 °C, due to the fact that some of vinyl alcohol segments were subject to dehydration to form a conjugated unsaturated structure,[21] and the other at 290 °C in the range 250–330 °C, resulting from melting of crystallites. Although it has been reported that marked dehydration might occur at 300 °C,[22] which is within this temperature range, the TGA results in Figure 6a indicate that this was not the case since no appreciable further weight loss was observed. As the PVA was treated with HBF_4, the dehydration peak shifted from 220 °C to 165 °C, as was also observed by Dunn et al.,[23] and the melting of the crystallite peak at 290 °C disappears. The above-mentioned acid-treated PVA was prepared by immersing the PVA film in 1.2 M HBF_4 aqueous solution for 12 h and was then dried under dynamic vacuum pumping for more than 1 day.

For e-PAn/PVA, the characteristic peaks at 220 and 295 °C can be ascribed to pure PVA, and the peak at 160 °C can be assigned to the acid-treated PVA. In addition, a new peak at 355 °C was observed (Figure 5c) and Table III). To clarify the nature of these new peaks, we also prepared a physical blend of PAn/PVA (b-PAn/PVA) by grinding PVA aqueous solution with e-PAn powder of weight ratio 1/1.2 to give a well-mixed blend, casting into a film, and finally drying under dynamic vacuum pumping for 1 day. Since there is no peak at 355 °C for b-PAn/PVA, the new peak of the composites must result from a breakage of the graft bond.

c-PAn/PVA has nearly the same characteristic peaks as those of e-PAn/PVA (Figure 5c and Table III), but the relative size of the peak at 220 °C to that at 295 °C is

Table III
Characteistic Value (°C) of the DSC Curves in Figure 5

Figure 5 sample[a]	acid-catalyzed dehydration of PVA	dehydration of PVA	crystallite melting of PVA	evaporation of acid	breakage of graft bond
(a) e-PAn				300	
e-PAn (undoped)					
(b) PVA		220	290		
PVA (acid treated)	165				
(c) e-PAn/PVA	160	220	295	295	355
c-PAn/PVA	170	220	285	285	355
b-PAn/PVA		215	300 (br)	300 (br)	

[a] e, c, and b refer to electrochemical, chemical, and blending, respectively.

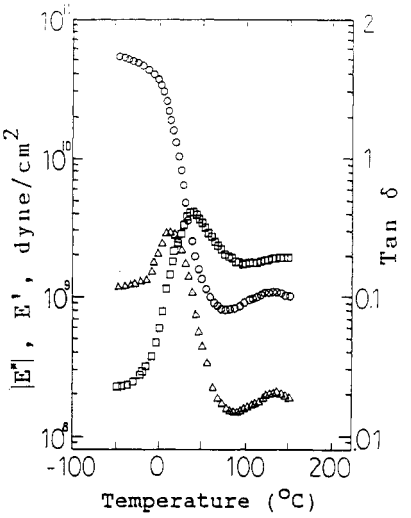

Figure 7. Dynamic mechanical measurements on the PVA film: tensile modulus $|E^*|$ (○); tensile loss modulus E'' (△); tan δ (□).

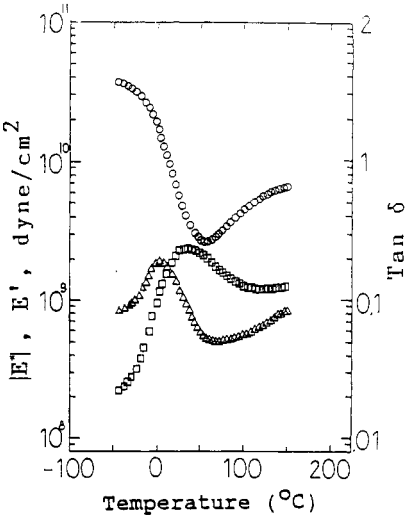

Figure 8. Dynamic mechanical measurements on the c-PAn/PVA film: tensile modulus $|E^*|$ (○); tensile loss modulus E'' (△); tan δ (□).

opposite that of e-PAn/PVA. The peak of dehydration of PVA in e-PAn/PVA was significantly larger than that in c-PAn/PVA.

5. Dynamic Mechanical Measurements. Dynamic mechanical measurements for PVA, e-PAn/PVA, and c-PAn/PVA are shown in Figures 7–9. The specimens were stored in a desiccator with silica gel before use, but were not subjected to dynamic vacuum pumping for removal of the residual moisture. Complete removal of water would lead to a brittle specimen, which might break during a dynamic mechanical measurement. The characteristic transition temperatures at maximum tan δ are

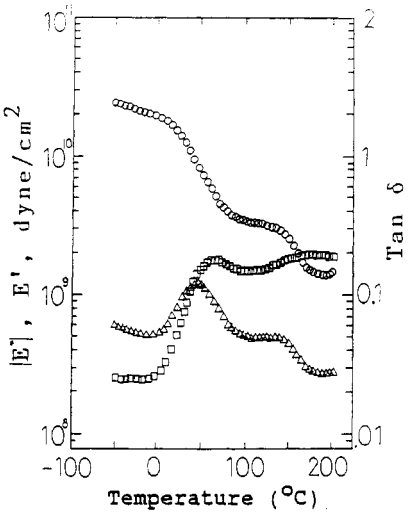

Figure 9. Dynamic mechanical measurements on the e-PAn/PVA film: tensile modulus $|E^*|$ (○); tensile loss modulus E'' (△); tan δ (□).

Table IV
Characteristic Values of the Dynamic Mechanical Measurements in Figures 7–9

	$T_{g,l}$,[a] °C		$T_{g,h}$,[a] °C	
	from tan δ	from E''	from tan δ	from E''
PVA	36	12	135	135
c-PAn/PVA	36	2		
e-PAn/PVA	65	44	177	141

[a] $T_{g,l}$ and $T_{g,h}$ refer to the temperatures at the maximum $|E^*|$, E'', and tan δ.

listed in Table IV.

For PVA, tan δ shows T_g at 36 °C, lower than that normally observed at 65 °C (Figure 7). This is due to the plasticizing effect caused by the presence of about 3.5–9.8% moisture as can be estimated from the TGA curve of PVA (Figure 6a). The occurrence of a maximum in $|E^*|$, E'' and tan δ at 135 °C can be attributed to a competition between an increase in $|E^*|$ due to the evaporation of water and a decrease in $|E^*|$ due to the increase of temperature. This is in agreement with the presence of the first peak at 125 °C in the DSC measurement (Figure 5a), which is due to the evaporation of water. Dehydration has no contribution to the increase in $|E^*|$, since it occurs at a temperature higher than 165 °C and reaches a maximum at 213 °C (Figure 5b).

For c-PAn/PVA, the tan δ curve shows the presence of T_g at 36 °C (Figure 8), the same as that of pure PVA. This indicates that there exist some PVA domains not affected by the PAn in the composite. However, the tan δ peak is slightly broader than that of the pure PVA, which can be attributed to the hydrogen-bonding interaction and grafting at the boundaries between the PAn and PVA phases.

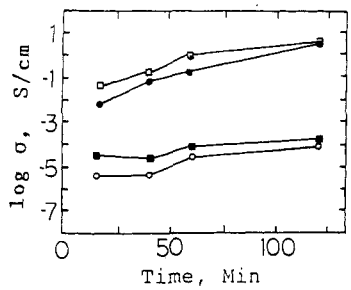

Figure 10. log (conductivity) versus reaction time of the e-PAn/PVA films: bulk value (□); the electrode side (●); the solution side (○); along the thickness direction (■).

The increase of $|E^*|$ with temperature after 50 °C can also be attributed to a continuous evaporation of water; the extent of increase is much greater than that of pure PVA due to the higher moisture content and the excess acid in this composite film (Figure 6a,b).

For e-PAn/PVA, the tan δ curve has two maxima, one at 65 °C and the other at 177 °C (Figure 9). The latter peak is rather broad and flat. The valley between these two peaks is very shallow. The first peak is higher than the T_g of PVA by 29 °C and can be attributed to the less-grafted PVA phase located in the region near the surface of the solution side, in which a smaller amount of PAn was generated, while the second broad peak can be attributed to the glass transition of the highly grafted PVA phase located at the region near the surface of the electrode side in which a much higher amount of PAn was generated. The elevation of T_g showed that the finely dispersed PAn synthesized by the electrochemical method in the composite has affected the chain movement of PVA. The shallow valley indicates a continuous gradient of local PAn content along the direction of thickness. This explanation is also supported by the presence of two rubbery plateaus in the $|E^*|$ curve. No increase in $|E^*|$ with temperature between 80 and 130 °C was observed, due to a lower moisture content in the sample than in c-PAn/PVA as can be seen in the TGA curves (Figure 6b,c). The first and second plateaus are associated with the phases with less-grafted and highly grafted PVA, respectively.

6. Conductivity Measurements. Conductivity measurements on the e-PAn/PVA composite (with drying in a desiccator only) at various polymerization times are shown in Figure 10. The conductivities of both surfaces were measured by the four-point method and those along the thickness direction by the two-disk method. The bulk conductivity measured by the sandwich type four-probe method was about 10^{-2} S/cm after 20 min of polymerization and increases to a constant level of about 5 S/cm after 1 h (Figure 10), which was about equal to that of PAn.

The conductivity of the film surface on the electrode side also increases with polymerization time and reaches the same level as PAn, indicating that the surface was covered with a layer of PAn, it is higher than that of the solution side by a factor of about 10^4. Along the thickness direction, the conductivity is lower than the bulk conductivity and is slightly higher than that of the surface of the solution side; this difference must be due to the gradient of PAn content along the thickness direction.

Variations of bulk conductivity with temperature of e-PAn, c-PAn/PVA, and e-PAn/PVA (all three samples were dried by storage in a desiccator only) are shown in Figure 11. The conductivities increase with temperature below room temperature but decrease slowly above room temperature for e-PAn and c-PAn/PVA. For e-PAn/PVA the conductivities drop significantly from 50 to 75 °C and then decrease slowly as temperature increases. The

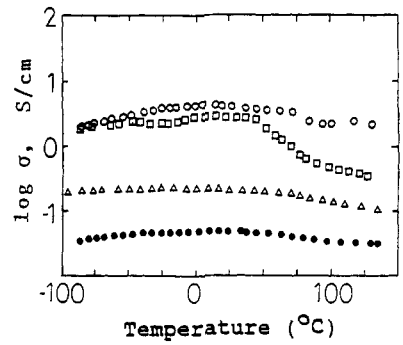

Figure 11. log (conductivity) versus temperature of e-PAn and PAn/PVA films: e-PAn (○), c-PAn/PVA (△), and e-PAn/PVA (□) with drying in the desiccator only; e-PAn/PVA after drying under vacuum (●).

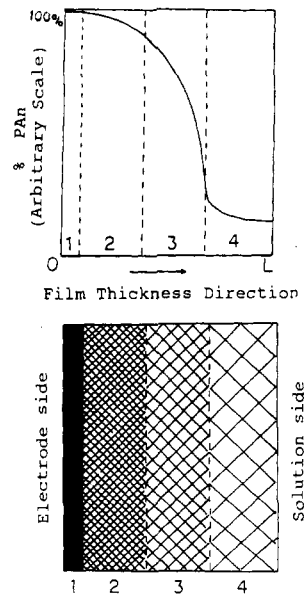

Figure 12. PAn content profile and morphological structure in the e-PAn/PVA film: (1) PAn layer; (2) PAn-rich layer; (3) gradient PAn content layer; (4) PAn-poor layer.

decreases of conductivity with temperature for the former two cases can be attributed to the decrease in moisture content, which could vary the interaction between the dopant and PAn.[24,25] The significant drop of conductivity in e-PAn/PVA can be attributed to the presence of moisture in the PAn-free PVA phase and to the characteristic of PAn content gradient along the thickness direction, since this sudden drop was not present for e-PAn/PVA after drying under vacuum and for c-PAn/PVA without further drying under vacuum (Figure 11).

Morphological Structure of the Composite Films

From the studies above, the morphological structure of e-PAn/PVA can be represented by four regions as shown in Figure 12. On the surface of the electrode side, there is a dense layer of PAn (region 1, PAn layer). Below this layer, there are PAn fibrilar networks dispersed in the PVA matrix with considerable uniformity (region 2, PAn-rich layer). Parts of the PAn chains are grafted onto the PVA chains. Next to region 2, the local content of PAn decreases along the thickness direction (region 3, gradient layer). In the region close to the surface of the solution side, the PAn content levels off (region 4, PAn-poor layer). Such a structure would naturally lead to a conductivity gradient along the thickness direction.

For c-PAn/PVA composite film, the PAn content on the two surfaces is the same. A PAn composition gradient toward the center of the film can be expected for a short

polymerization time. For long polymerization time, the PAn distribution in the film may become uniform.

Acknowledgment. We thank the National Science Council of the ROC for financial aid through the project "Studies on Conducting Polymers" (NSC 76-0405-E007-01).

References and Notes

(1) MacDiarmid, A. G.; Chiang, J. H.; Halpern, M.; Huang, W. S.; Mu, S. L.; Somasiri, N. L. D.; Wu, W.; Yaniger, S. I. *Mol. Cryst. Liq. Cryst.* **1985**, *121*, 173.
(2) Travers, J. D.; Chroboczek, J.; Devreux, F.; Genoud, F.; Nechtschein, N.; Syed, A.; Genies, E. M.; Tsintavis, C. *Mol. Cryst. Liq. Cryst.* **1985**, *121*, 195.
(3) Mohilner, D. M.; Adams, R. N.; Argensinger, W. J. *J. Am. Chem. Soc.* **1962**, *84*, 3618.
(4) Genies, E. M.; Syed, A. A.; Tsintavis, C. *Mol. Cryst. Liq. Cryst.* **1985**, *121*, 181.
(5) Kitani, A.; Izumi, J.; Yano, J.; Hiromoto, Y.; Suzuki, K. *Bull. Chem. Soc. Jpn.* **1984**, *57*, 2254.
(6) Carlin, C. M.; Kepley, L. J.; Bard, A. J. *J. Electrochem. Soc.* **1985**, *132*, 353.
(7) Wang, B.; Tang, J.; Wang, F. *Synth. Met.* **1986**, *13*, 329.
(8) Chen, S. A.; Lee, T. S. *J. Polym. Sci., Polym. Lett. Ed.* **1987**, *25*, 455.
(9) Zuo, F.; McCall, R. P.; Ginder, J. M.; Roe, M. G.; Leng, J. M.; Epstein, A. J.; Asturias, G. E.; Ermer, S. P.; Ray, A.; MacDiarmid, A. G. *Synth. Met.* **1989**, *29*, E445.
(10) DePaoli, M. A.; Waltman, R. J.; Diaz, A. F.; Bargon, J. *J. Polym. Sci., Polym. Chem. Ed.* **1985**, *23*, 1687.
(11) Niwa, O.; Kakuchi, M.; Tamamura, T. *Macromolecules* **1987**, *20*, 749.
(12) Niwa, O.; Kakuchi, M.; Tamamura, T. *Polym. J.* **1987**, *19*, 1293.
(13) Ojio, T.; Miyata, S. *Polym. J.* **1986**, *18*, 95.
(14) Yosomiya, R.; Hirata, M.; Haga, Y.; An, H.; Seki, M. *Makromol. Chem., Rapid Commun.* **1986**, *7*, 697.
(15) Pei, Q.; Bi, X. *J. Appl. Polym. Sci.* **1989**, *38*, 1819.
(16) Rembaum, A. *Encyclopedia of Polymer Science and Technology*; Mark, H., Ed.; John Wiley: New York, 1972; Vol. 11, p 320.
(17) Brahma, S. K. *Solid State Commun.* **1986**, *57*, 673.
(18) Harada, I.; Furukawa, Y. *Synth. Met.* **1989**, *29*, E303.
(19) Furukawa, Y.; Ueda, F.; Hyodo, Y.; Harada, I.; Nakajima, T.; Kawagoe, T. *Macromolecules* **1988**, *21*, 1297.
(20) Pouchert, C. J. *The Aldrich Library of Infrared Spectra*, 2nd ed.; Aldrich Chemical Company: Milwaukee, WI, 1978; p 555.
(21) Tsuchiya, Y.; Sumi, K. *J. Polym. Sci.* **1969**, *A-1* (7), 3151.
(22) Gelfman, A. Y.; Bidnaya, D. S.; Sigalova, L. L.; Buravleva, M. G.; Koba, V. S. *Dokl. Phys. Chem. (Engl. Transl.)* **1964**, *154*, 125.
(23) Dunn, A. S.; Coley, R. L.; Duncalf, B. In *Properties and Applications of Polyvinyl Alcohol*; Finch, C. A., Ed.; Monograph No. 30; Society of Chemical Industry: London, 1968; p 208.
(24) Alix, A.; Lemoine, V.; Nechtschein, M.; Travers, J. P.; Menardo, C. *Synth. Met.* **1989**, *29*, E457.
(25) Javadi, H. H. S.; Angelopoulous, M.; MacDiarmid, A. G.; Epstein, A. J. *Synth. Met.* **1989**, *29*, E409.

Registry No. PAn (homopolymer), 25233-30-1; PVA (homopolymer), 9002-89-5; (PAn)(PVA) (graft copolymer), 131761-23-4; HBF_4, 16872-11-0.